Developmental Cell
Article

Extracellular Matrix Protein Anosmin Promotes Neural Crest Formation and Regulates FGF, BMP, and WNT Activities

Yukinori Endo,[1,*] Hiroko Ishiwata-Endo,[1] and Kenneth M. Yamada[1,*]
[1]Laboratory of Cell and Developmental Biology, National Institute of Dental and Craniofacial Research, National Institutes of Health, Bethesda, MD 20892-4370, USA
*Correspondence: yukinorishiko@yahoo.co.jp (Y.E.), kenneth.yamada@nih.gov (K.M.Y.)
http://dx.doi.org/10.1016/j.devcel.2012.07.006

SUMMARY

Neural crest cells are a transient stem cell-like population appearing during vertebrate embryonic development. Generation of the cranial neural crest is known to require a balanced combination of FGF and BMP levels. However, it is poorly understood how the functions of such growth factors are controlled in the extracellular space. Anosmin is an extracellular matrix protein implicated in FGF signaling and mutated in Kallmann syndrome. Here, we demonstrate that anosmin is synthesized locally in the cranial neural crest of chicken embryos and is essential for cranial neural crest formation. Anosmin upregulates *FGF8* and *BMP5* gene expression; it also enhances FGF8 activity while inhibiting BMP5 and WNT3a signaling. Taken together, our data establish that the matrix protein anosmin is required for cranial neural crest formation, with functional modulation of FGF, BMP, and WNT.

INTRODUCTION

Understanding how the constituents of cellular microenvironments containing extracellular matrix (ECM) and secreted regulatory factors are coordinated to promote specific tissue differentiation is one of the major challenges in cell and developmental biology. Recently, important roles of local ECM molecules have been suggested in tissue/organ morphogenesis and stem cell fate determination (Sakai et al., 2003; Wang et al., 2008; Engler et al., 2006). The composition and stiffness of the local microenvironment affect fate determination, differentiation, proliferation, survival, polarity, and migration of cells (reviewed in Hynes, 2009; Yamada and Cukierman, 2007; Nelson and Bissell, 2006). Furthermore, local interactions and matrix-mediated presentation of secreted growth factors to cell surface receptors are also important during embryonic development, stem cell fate determination, and cancer (e.g., see reviews by Hynes, 2009; Discher et al., 2009). Thus, it is important to understand how growth factor cues that govern tissue differentiation are coordinated by the microenvironment.

Neural crest cells appear transiently during embryonic development, and they generate a variety of cells and tissues including neurons, glia, and craniofacial bones and connective tissues (Le Douarin and Kalcheim, 1999). The neural crest primordium forms at the boundary of the epidermal ectoderm and neural plate; it is specified by local growth factors such as fibroblast growth factor (FGF), bone morphogenetic protein (BMP), and Wingless/INT-related (WNT) during gastrulation (Basch et al., 2006). Furthermore, it has been suggested that a balance between the levels of FGF and BMP (an intermediate level of the latter) is important for cranial neural crest generation (reviewed in Sauka-Spengler and Bronner-Fraser, 2008). Specification and formation of the neural crest involves a variety of transcription factors, including the paired box transcription factor PAX7, zinc finger transcription factor SNAI2, forkhead transcription factor FOXD3, and HMG box transcription factor SOX9 (Basch et al., 2006; Nieto et al., 1994; Dottori et al., 2001; Cheung and Briscoe, 2003). These transcription factors are induced by growth factors, and they promote not only neural crest specification/formation but also subsequent epithelial-mesenchymal transition (EMT) and cell migration into the embryonic body (reviewed in Sauka-Spengler and Bronner-Fraser, 2008).

During neural crest cell development, ECM molecules such as fibronectin, laminin, and collagen have been studied extensively for their roles in cell migration and differentiation (reviewed in Henderson and Copp, 1997; Rogers et al., 1990). Recent studies suggest that ECM molecules, as well as growth factor antagonists, can be involved in achieving specific tissue differentiation. For example, the olfactomedin family has been identified as a new class of regulatory extracellular proteins, with the olfactomedin family member Noelin-1 enhancing neural crest formation in chick development (Barembaum et al., 2000) and ONT1 involved in *Xenopus* dorsal-ventral (DV) axis formation by controlling protein levels of chordin, a BMP antagonist (Inomata et al., 2008). However, it is poorly understood how ECM proteins might coordinate functions of growth factors such as FGF, BMP, and WNT during embryonic development. Consequently, we hypothesized that ECM molecules might regulate cranial neural crest formation by controlling functions of these growth factors in local microenvironments.

In this study, we identified the ECM protein anosmin as a molecule closely linked by both temporal and spatial mRNA expression patterns with formation of the cranial neural crest. Loss- and gain-of-function experiments using antisense morpholino oligonucleotides (mo) or purified anosmin protein and

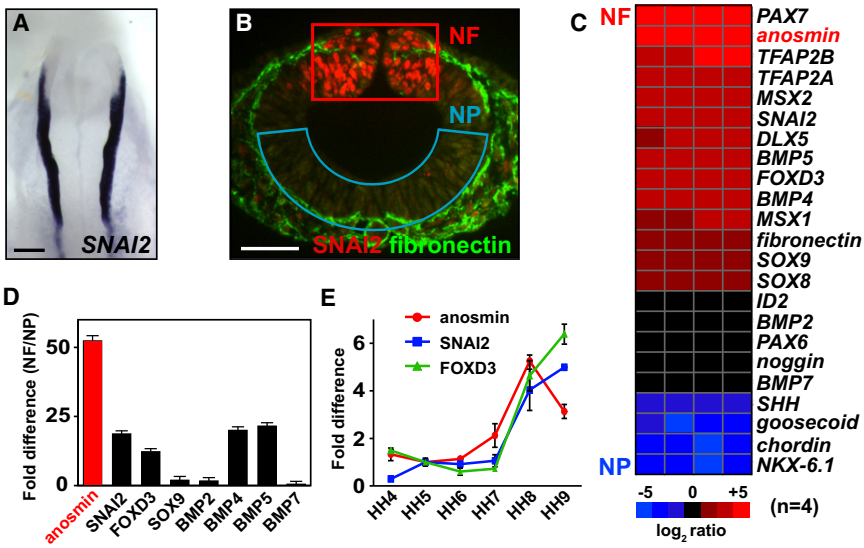

Figure 1. Identification of Anosmin Gene Expression in NFs

(A) *SNAI2* mRNA expression in NFs of chicken embryo during neural crest formation (HH8). Scale bar, 150 μm.

(B) Cross-section of cranial region of a HH8 embryo coimmunostained with SNAI2 and fibronectin antibodies. NF (red rectangle) and NP (blue arc) were dissected from HH8 embryos (80 to 114 embryos, n = 4), and total RNA was analyzed using GeneChip chicken genome arrays (32,773 transcripts corresponding to >28,000 chicken genes, Affymetrix). Scale bar, 150 μm.

(C) Gene expression profiles in NF and NP by microarray analysis. Cluster analysis was performed using $\log_2$ ratios for NF and NP genes.

(D) Fold difference (NF/NP) of *anosmin* gene expression compared with neural crest genes and *BMP* family genes by quantitative PCR (qPCR). Data are shown as means and SEM.

(E) Time-dependent change of *anosmin* gene expression compared with *SNAI2* and *FOXD3* from HH4 to HH9 by qPCR (HH5 gene expression is 1). Data are shown as means and SEM.

growth factors reveal that anosmin plays a critical role in cranial neural crest formation. Using growth factor-specific luciferase reporters, we show that anosmin specifically enhances FGF8 functions while inhibiting BMP5 and WNT3a. Based on these findings, we propose that anosmin promotes cranial neural crest formation by governing growth factor functions in avian embryonic development.

RESULTS

Microarray Analysis Identifies the ECM Protein Anosmin in the Neural Fold

During neurulation in chicken embryos, the cranial neural fold (NF) is a unique structure formed at the boundary of the neural plate and the epidermal ectoderm. The neural fold gives rise to the cranial neural crest, which is characterized by expression of *SNAI2* messenger RNA (mRNA) and protein (Figures 1A and 1B). The ECM protein fibronectin is localized mainly in the basement membrane and mesenchymal tissues rather than in the neural fold (Figure 1B). We searched for an ECM protein that was synthesized locally in the neural fold with the hypothesis that this type of ECM protein might regulate neural crest formation. We analyzed gene expression profiles of the NF compared to the ventral neural plate (NP; Figure 1B) from embryos at the cranial neural crest formation stage (Hamburger & Hamilton stage 8; HH8) using chicken genome microarray chips from Affymetrix; the microarray data are deposited in GEO under series accession number GSE38381.

We first validated the microarray data by searching for differential expression of known neural crest genes such as *SNAI2*, *FOXD3*, and *SOX9* compared with neural plate genes such as *SHH*, *chordin* and *NKX-6.1* (Figure 1C). We confirmed that the neural fold differential gene expression profiles included a set of 10 known neural crest genes with high differential expression (Figure 1C). After this validation, we found that extracellular matrix gene *anosmin* was prominent in the neural fold profiles and displayed the highest fold difference ($\log_2$ ratio > 5.7; Figure 1C) compared to other extracellular matrix genes (e.g., *fibronectin*, $\log_2$ ratio = +1.9, and *laminin* and *collagen* showed no significant differences; data not shown). We confirmed the differential gene expression of anosmin by reverse transcription PCR (data not shown) and quantitative PCR (qPCR; Figure 1D). Comparable to known neural crest regulatory genes, such as *SNAI2*, *FOXD3*, *SOX9*, and *BMP* family genes, *anosmin* was expressed more than 50 times higher in the neural fold than in the neural plate by qPCR (Figure 1D), and the peak of anosmin expression was at HH8 (Figure 1E). Human *anosmin* gene mutations cause the X-linked form of Kallmann syndrome (KAL1; Legouis et al., 1991) and result in anosmia and craniofacial defects. It has recently been suggested that anosmin modulates FGF signaling (Hu et al., 2009). However, it is poorly understood how anosmin functions during embryonic development. This study identifies functions of anosmin in cranial neural crest development.

Anosmin Is Specifically Expressed in the Cranial Neural Crest

We first characterized the spatial and temporal patterns of craniofacial *anosmin* mRNA expression by in situ hybridization (Figures 2A–2I) compared to the neural crest marker *SNAI2* (Figures 2J and 2K). *Anosmin* mRNA expression first appeared in the anterior neural ridge (ANR) at HH5$^+$ (Figure 2B, arrowheads). At HH6-7$^+$, its expression extended to more central regions of cephalic neural fold (Figures 2C and 2D, arrowheads), and by HH8 and 9$^-$, its expression was specifically and strongly localized to the entire NF (Figure 2F, arrowheads). As determined by serial sections, *anosmin* mRNA localization overlapped with the dorsal zone of *SNAI2* expression (Figures 2G and 2J, arrowheads), suggesting that the dorsal part of the cranial neural crest and the ANR are the primary sources of anosmin. However, during or after neurulation (just before the time of neural crest cell emigration at HH9$^-$ to 9), *anosmin* mRNA expression levels progressive decreased in the NFs (Figures 2I and 2E, arrowheads).

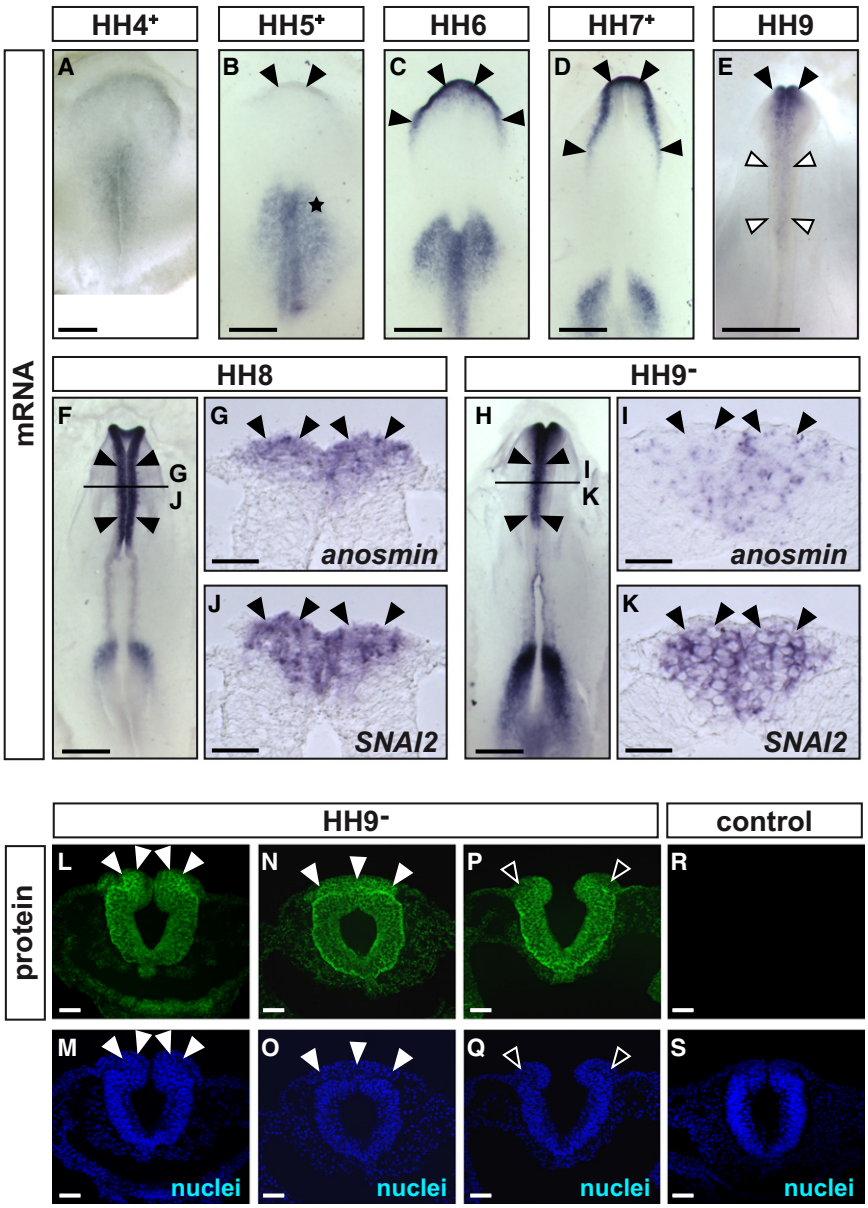

Figure 2. *Anosmin* mRNA and Protein Expression in NF

(A–K) *Anosmin* mRNA expression by whole-mount in situ hybridization. Weak *anosmin* expression is detected in the ANR at HH5^{+} (B, indicated with arrowheads), and then its expression expands progressively from HH6 to HH8 to cover the NF, as indicated with arrowheads in (C), (D), and (F). By the time of neural crest migration, *anosmin* expression is decreased (E, indicated with white arrowheads). *Anosmin*, in (G) and (I), and *SNAI2*, in (J) and (K), mRNA expression on a series of serial sections by in situ hybridization. *Anosmin* expression is colocalized with *SNAI2* in NF at HH8, indicated by arrowheads in (G) and (J), but at HH9^{-} *anosmin* expression begins to decrease at the anterior/posterior midbrain region indicated by arrowheads in (H), (I), and (K). Scale bar, 150 μm in (A)–(F) and (H) and 50 μm in (G), (I), (J), and (K). (L–S) Anosmin protein expression in the anterior midbrain region (L, at the same level as the upper arrowheads in H), posterior midbrain region (N), and midbrain/hindbrain boundary region (P, same level as lower arrowheads in H) of HH 9^{-} embryo. Before neural crest migration, anosmin is present in the entire neural plate with highest expression in the neural fold (L, indicated by arrowheads). Arrowheads indicate anosmin expression in cranial neural crest cells emigrating from cranial neural tube (N). At the midbrain/hindbrain boundary region, anosmin protein expression is weaker compared with the anterior midbrain regions (P, indicated by open arrowheads). As a negative control, preimmune serum was used on sections of HH9 embryos (R). Asterisk in (B) indicates migrating mesenchymal cells of primitive streak and presomitic mesoderm. Nuclei were stained by DAPI, as shown in (M), (O), (Q), and (S). Scale bar, 50 μm.
See also Figure S1.

Next, we determined the localization of anosmin protein using an affinity-purified polyclonal antibody against chicken anosmin (Figures 2L, 2N, and 2P; Figure S1 available online). We found that anosmin protein extended into the entire cranial neural ectoderm but with highest expression in the neural fold of the anterior midbrain (Figure 2L, arrowheads) and with lower expression in the posterior midbrain (Figure 2P, open arrowheads) before neural crest cell emigration. At the time of neural crest cell migration, anosmin protein was also expressed in the neural crest cells (Figure 2N, arrowheads). As previously reported by Hardelin et al. (1999), anosmin protein was localized in basement membranes and interstitial spaces of the ectoderm. This regional and transient expression of *anosmin* mRNA and the presence of anosmin protein suggested that anosmin could be involved in cranial neural crest formation.

Anosmin Is Needed for Cranial Neural Crest Formation

To examine whether anosmin is required for cranial neural crest formation, we introduced antisense mo into the cranial ectoderm of HH4^{+}-5 embryos to inhibit new synthesis of anosmin protein in NFs (see Experimental Procedures). After introduction of mo, the embryos were cultured for 10–12 hr until HH8-9. Compared with control-mo, anosmin-mo produced approximately 50% knockdown of anosmin protein in NFs (Figures S2A–S2F). In control-mo-treated embryos, *SNAI2* mRNA was expressed normally in the neural crest (Figures 3A and 3B). In contrast, *SNAI2* expression was substantially decreased in anosmin knockdown embryos compared with controls (Figures 3B and 3D, 6 out of 6, arrowheads). We also examined the effects of anosmin knockdown on other neural crest markers by qPCR (Figures 3I–3O). qPCR confirmed the results for *SNAI2*, accompanied by reductions of *FOXD3*, *SOX9*, and *MSX1* (>50%; Figures 3J–3L) in NF, while levels of expression of *PAX7*, *TFAP2A*, and *PAX6* were not changed (Figures 3M–3O). Because *PAX7*

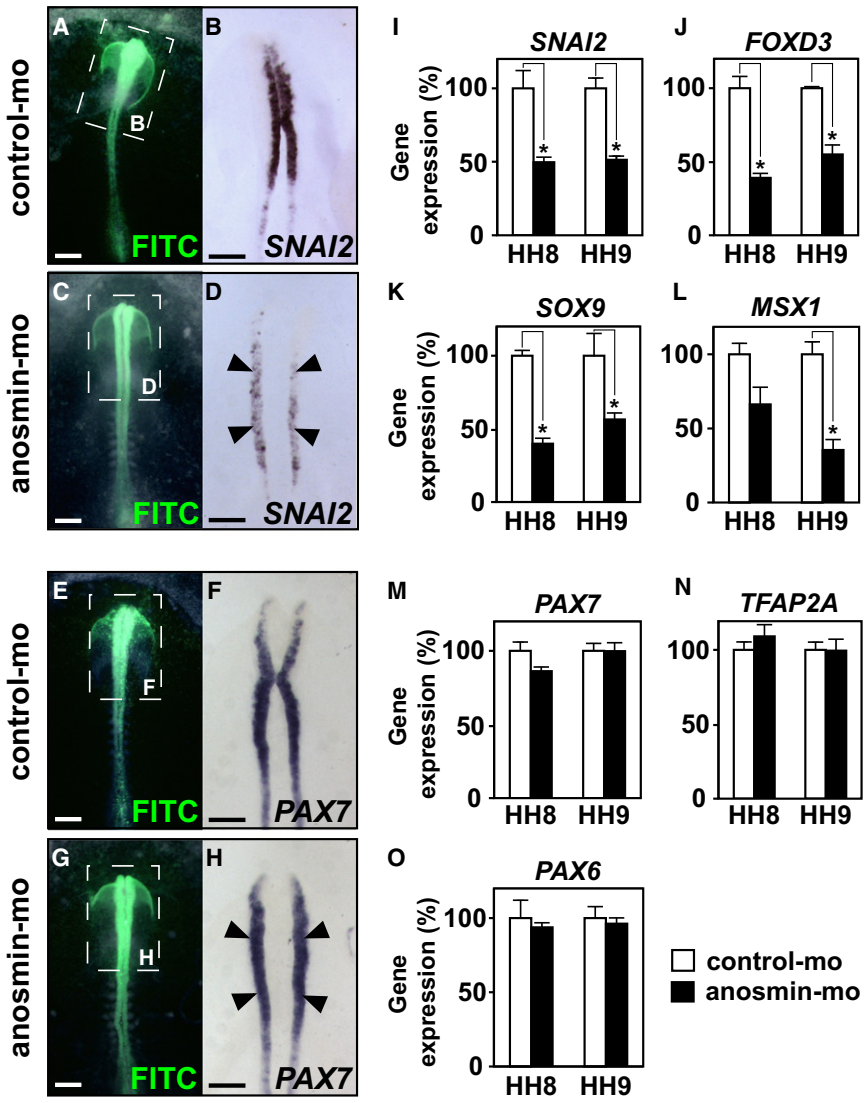

Figure 3. Reducing Anosmin in the Neural Fold Decreases *SNAI2* but Not *PAX7* Expression

(A–H) Electroporations of FITC-tagged control-mo, in (A), (B), (E), and (F), or FITC-tagged anosmin-mo, in (C), (D), (G), and (H), were performed using HH4^{+}-5 embryos, and the embryos were cultured for 10–11 hr until HH8-9. Transfected regions are visualized by FITC fluorescence overlaid on brightfield images of live embryos in (A), (C), (E), and (G). *SNAI2* and *PAX7* expression in the head fold, in (B), (D), (F), and (H), are shown at higher magnification corresponding to the boxed areas of (A), (C), (E), and (G), respectively. In anosmin-mo-treated embryos, *SNAI2* expression was decreased (D, indicated by arrowheads), but *PAX7* expression was not changed significantly (H, indicated by arrowheads). Scale bar, 200 μm. (I–O) Gene expression of neural fold genes by qPCR. NFs of HH8 and HH9 control-mo- (each n = 3) or anosmin-mo-treated embryos (each n = 3) were dissected, and total RNA was used for qPCR. *SNAI2*, *FOXD3*, *SOX9*, and *MSX1* expression levels were decreased in anosmin knockdown neural fold in (I), (J), (K), and (L), while *PAX7*, *TFAP2A*, and *PAX6* expression did not change significantly, as shown in (M), (N), and (O). Data are shown as means and SEM. *$p < 0.01$.
See also Figure S2.

gene expression is required for neural crest specification during gastrulation (Basch et al., 2006), we confirmed the qPCR results by whole-mount in situ hybridization (Figures 3E–3H) Compared with control-mo-treated embryos, *PAX7* expression of anosmin-mo-treated embryos showed no significant difference (Figures 3F and 3H, 5/5, arrowheads). Apoptosis was not increased in anosmin-depleted embryos (Figure S2G), and the decreased expression of *SNAI2* and *FOXD3* was rescued by injection of exogenous anosmin (Figures S2H and S2I). Combined with the anosmin gene expression patterns, our findings suggest that anosmin is needed for cranial neural crest formation rather than for initial neural crest specification.

FGF8 and *BMP5* Expression in NF Requires Anosmin

We hypothesized that anosmin might play regulatory roles in vivo—particularly roles related to the proposed requirements for FGF and an intermediate level of BMP in cranial neural crest formation (reviewed in Sauka-Spengler and Bronner-Fraser, 2008). We first examined whether anosmin knockdown might affect expression of either of these growth factors during neural crest formation.

FGF8 is known to play an important role in cranial neural crest formation and head development (Litsiou et al., 2005; Hong et al., 2008; Monsoro-Burq et al., 2005). In chicken embryos, *FGF8* is expressed strongly in the ANR and in cranial neural crest (Bailey et al., 2006; Figure 4B). We examined for altered *FGF8* expression in NFs of anosmin knockdown embryos by whole-mount in situ hybridization. We found that *FGF8* expression was substantially decreased in the NF compared with controls (Figure 4D, 4/4, arrowheads). We quantified the decrease in *FGF8* expression in neural folds of anosmin-mo embryos by qPCR as >60%, compared to controls (Figure 4E). These results suggest that *FGF8* is a gene downstream of anosmin required for cranial neural crest formation.

We next examined for regulatory effects of anosmin on the BMP family. Our gene expression profiles of NF identified high differential expression of *BMP4* and *BMP5* mRNA (Figure 1C), and this high expression was confirmed by qPCR (Figure 1D). We used whole-mount in situ hybridization to characterize the temporal and spatial expression pattern of *BMP5* in cranial neural crest (Figure S3). *BMP5* expression was first detected in cranial neural crest at HH7 (Figure S3A, arrowheads) after *SNAI2* expression appeared at HH6 (Endo et al., 2002; data not shown); *BMP5* was then strongly expressed in the cranial

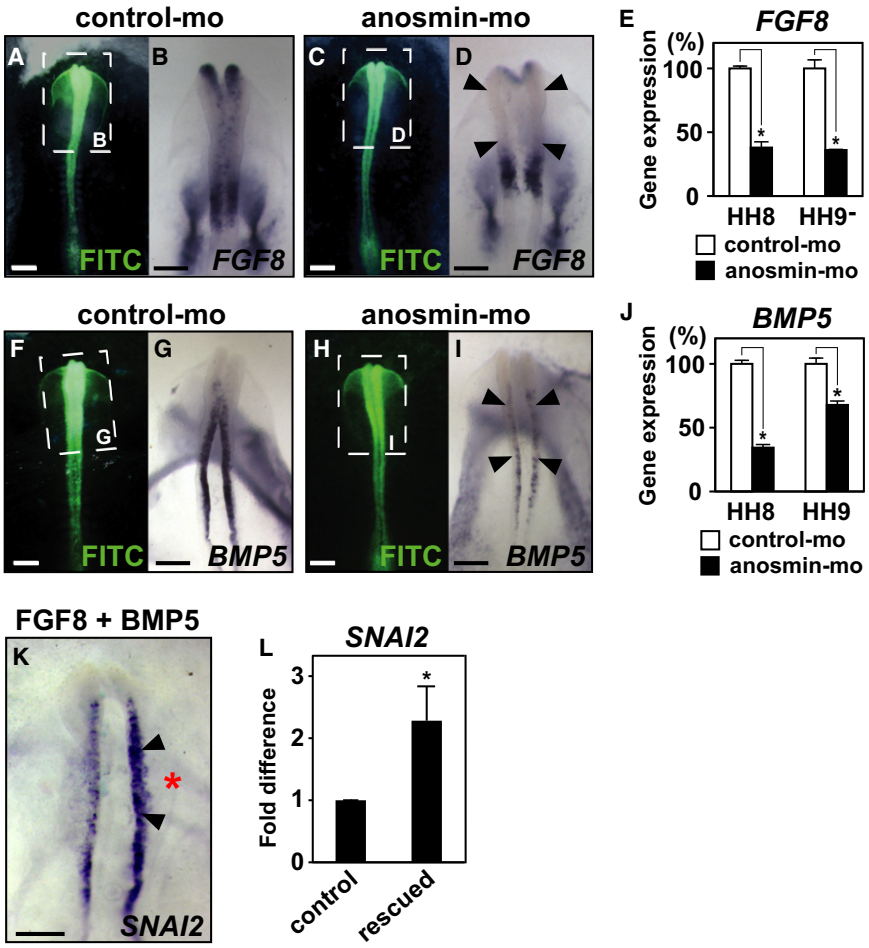

Figure 4. Anosmin Is Required for *FGF8* and *BMP5* Expression in NF

(A–J) Electroporation of FITC-tagged control-mo (A, B, F, and G) and FITC-tagged anosmin-mo (C, D, H, and I) was performed using HH4^{+}-5 embryos, and the embryos were cultured for 10-11 hr until HH8-9. Transfected regions are shown as FITC fluorescence overlaid on the brightfield image of live embryos in (A), (C), (F), and (H). *FGF8* and *BMP5* expression in the head fold are shown at higher magnification in (B), (D), (G), and (I), corresponding to the boxed areas of (A), (C), (F), and (H), respectively. Coincident with the qPCR results (E and J), expression of *FGF8* and *BMP5* was decreased in anosmin-mo-treated embryos (D and I, indicated by arrowheads). Gene expression of neural fold genes by qPCR is shown in (E and J). NFs of HH8 and HH9^{-} or HH9 embryos treated with control-mo (each n = 3) or anosmin-mo (n = 3) were dissected, and total RNA was used for qPCR. Expression of *FGF8* and *BMP5* were decreased in anosmin knockdown neural fold compared with controls. Data are shown as means and SEM. Scale bar, 200 μm. *p < 0.001.

(K and L) Rescue of *SNAI2* expression by FGF8 + BMP5 in anosmin-mo treated embryos. Electroporation of FITC-tagged mo was performed at HH4^{+}-5, and 6.5 hr after electroporation, a mixture of FGF8 (2 μg/ml) and BMP5 (10 μg/ml) proteins in 0.1% BSA/HBSS was injected into the right side (red asterisk) of the cranial regions of HH7^{+}-8^{-} embryos. The embryos were cultured for another 5.5 hr until HH8-9, and *SNAI2* expression was examined by whole-mount in situ hybridization. Compared with the internal control (left side), *SNAI2* expression was rescued on the right side (K, indicated by arrowheads). *SNAI2* expression in NFs from the control or rescued sides were quantified by ImageJ (L, each n = 4). Scale bar, 200 μm. Data are shown as means and SEM. *p < 0.02. See also Figure S3.

neural crest at HH8^{-}-9 (Figures S3B–S3D, arrowheads). In contrast, during cranial neural crest formation in chicken embryos, expression of *BMP2* and *BMP4* was downregulated in cranial neural crest (Endo et al., 2002; data not shown). These results suggest that BMP5 is involved in cranial neural crest formation but not in its initial specification. Although the function of BMP5 in cranial neural crest formation has been not examined in detail, as previously shown for induction of *SNAI2* and *MSX2* expression in chicken limb development (Zuzarte-Luís et al., 2004), we also found that purified BMP5 protein upregulated/enhanced neural crest gene *MSX2* expression in NF and plate (data not shown).

We found that *BMP5* expression was clearly decreased in anosmin-mo-treated neural folds by whole-mount in situ hybridization (Figure 4I, 3/3, arrowheads). We quantified the decreases by qPCR (>50%, Figure 4J). In contrast, *BMP4* expression was not affected after anosmin knockdown according to qPCR (data not shown). Taken together, our results suggest that anosmin is required specifically for *BMP5* gene expression, as well as for other neural crest genes such as *SNAI2*, *FOXD3*, and *SOX9*, but not *BMP4*.

Anosmin Regulates Both FGF8 and BMP5 Required for Cranial Neural Crest Formation

FGF and BMP signaling are known to be required for both cranial neural crest specification and formation (Stuhlmiller and García-Castro, 2012; Mayor et al., 1997; Monsoro-Burq et al., 2003; Endo et al., 2002), which we confirmed using dominant-negative FGFR1 and noggin expression plasmids (data not shown). We tested whether FGF8 and BMP5 are required for cranial neural crest formation downstream of anosmin by a rescue experiment. We assayed for *SNAI2,* the key marker of neural crest formation, in anosmin-depleted embryos by injecting exogenous FGF8 or BMP5. Although neither FGF8 nor BMP5 alone could rescue (data not shown), very interestingly, injection of a certain combination of FGF8 (2 μg/ml) and BMP5 (10 μg/ml) proteins successfully restored normal expression of *SNAI2* on the injected side (Figure 4K, 8/10, arrowheads, and Figure 4L). In striking contrast, injection of FGF8 plus BMP5 protein into normal embryos never increased (and usually reduced) *SNAI2* expression (Figures S3H and S3H′, arrowheads). Moreover, bilateral injection into normal embryos of FGF8 or BMP5 did not increase *SNAI2* expression by qPCR, and FGF8 plus BMP5 strongly inhibited rather than

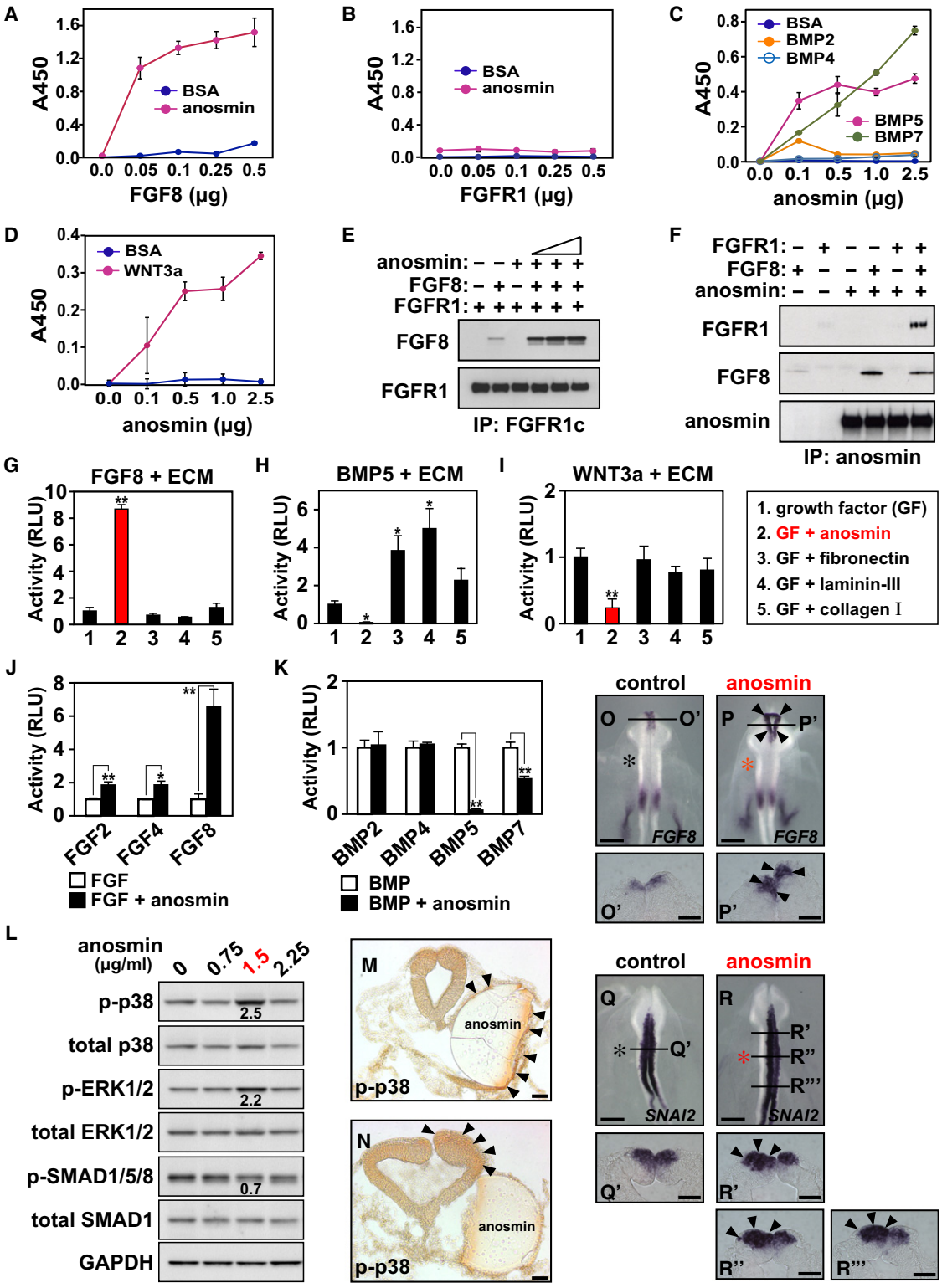

Figure 5. Purified Anosmin Protein Modulates FGF, BMP, and WNT Function by Direct Binding and Promotes Cranial Neural Crest Formation

(A–D) Anosmin binding to growth factors was examined by ELISA. (A-B) Wells were coated with tag-free purified recombinant anosmin protein or BSA as a control (5.0 μg/well), then incubated with the indicated amounts of FGF8 or FGFR1. (C-D) Purified recombinant anosmin (2.5 μg/well) was added to 96-well plates coated with various growth factors (0.5 μg/well) and BSA as a control. Bound anosmin was detected by anti-anosmin antibody (HL6157 or HL6308, see Supplemental Experimental Procedures), and binding was measured at 450 nm. Data are shown as means and SEM.

(E and F) Western blots of coimmunoprecipitation by FGFR1 (E) or anosmin (F) antibodies stained for FGF8 or FGFR1.

stimulated expression, underscoring the importance of an appropriate balance of growth factors (Figure S3I). These results indicate that *FGF8* and *BMP5* are downstream of anosmin, and all three molecules are required at appropriate levels for cranial neural crest formation.

Anosmin Modulates FGF, BMP, and WNT Activities

We then explored whether anosmin could directly alter FGF, BMP, and other growth factor activities beyond its function documented earlier in promoting gene expression. We produced recombinant chicken anosmin without any fusion protein tag using mammalian cells (Figure S1; see Supplemental Experimental Procedures). We first tested whether anosmin directly binds to growth factors using ELISA (see Supplemental Experimental Procedures). Anosmin bound strongly to FGF8, BMP5, BMP7, and WNT3a (Figures 5A, 5C, and 5D), yet anosmin did not directly bind to FGFR1, BMP2, or BMP4 (Figures 5B and 5C). In FGF8 ligand-binding assays (see Experimental Procedures for details), we confirmed that anosmin bound to FGF8 but not to FGFR1 (Figure 5F). In addition, however, anosmin increased the amount of FGF8 binding to FGFR1c in a dose-dependent manner (Figure 5E). The reverse experiment confirmed the conclusion that anosmin promotes FGF8-FGFR1 complex formation by direct binding to FGF8 (Figure 5F).

We next used a luciferase reporter assay system to test the effects of anosmin on FGF, BMP, and WNT signaling using mammalian cell lines stably expressing a promoter specific for each growth factor (see Experimental Procedures). We first confirmed that anosmin itself does not activate these assay systems, with no detectable effects on FGF, BMP, and WNT signaling in the absence of growth factors (data not shown). However, we found that, when combined with these growth factors, anosmin enhanced FGF8 activity more than 6-fold; FGF2 and FGF4 showed lower enhancement of approximately 2-fold (Figures 5G and 5J). When compared with other ECM molecules including fibronectin, laminin-III, and collagen I, anosmin specifically enhanced FGF8 activity; these other ECM proteins failed to enhance FGF8 activity (Figure 5G, compared to anosmin shown in red). In striking contrast, anosmin either inhibited or had no effect on BMP signaling; anosmin specifically inhibited BMP5 and BMP7 compared to BMP2 and BMP4 activities (Figure 5K). Interestingly, other ECM proteins such as fibronectin and laminin-III enhanced rather than inhibited BMP5 activity (Figure 5H, anosmin shown in red). Finally, anosmin inhibited WNT3a activity, whereas other ECM proteins had no significant effect on its activity (Figure 5I, anosmin shown in red). These results indicate that anosmin modulates FGF, BMP and WNT activities. Specifically, anosmin enhances FGF8 activity while inhibiting BMP5, BMP7, and WNT3a activity. Combined with ELISA assays and coimmunoprecipitation results, these results suggest that anosmin can function mechanistically to control specific extracellular growth factor activities through direct binding interactions to each of these molecules.

Exogenous Anosmin Promotes Phosphorylation of p38 In Vivo

We next examined whether anosmin can control downstream signaling molecules such as p38 and ERK1/2 MAP kinases or SMAD in vivo. Within 1–2 hr, p38 phosphorylation and ERK1/2 were enhanced 2.5 times and 2.2 times, respectively, while SMAD phosphorylation was inhibited 0.7 times by purified anosmin (1.5 μg/ml) in vivo (Figure 5L; Figure S4A). We confirmed the western blotting evidence for increased p38 phosphorylation by immunostaining. Normally, p38 is activated throughout the entire neural plate (data not shown). While control BSA beads had no effect on p38 phosphorylation, anosmin-soaked beads enhanced p38 phosphorylation in the cells surrounding the beads within 1–2 hr in vivo (21/23; Figure 5M, arrowheads). Moreover, we observed that p38-positive neural fold was expanded by this exogenous anosmin in forebrain (Figure 5N; Figures S4B and S4C, arrowheads, 7/9), whereas already established midbrain neural fold was unchanged compared with the contralateral side. These in vivo results are consistent with the in vitro findings that anosmin modulates growth factor activities.

Exogenous Anosmin Promotes Cranial Neural Crest Formation

We next examined whether experimental elevation of anosmin could promote cranial neural crest formation in vivo. We injected exogenous recombinant anosmin protein into NF regions and examined for enhanced expression of the key neural crest marker *SNAI2* by whole-mount in situ hybridization. Purified anosmin protein was injected into $HH7^+$ (2–3 somite-stage) embryos, and the embryos were allowed to develop until

(G–K) Luciferase activity expressed as relative luciferase units (RLU), with activity of each growth factor (GF) alone normalized to 1 RLU. For assaying FGF activity, mouse myoblasts (C2C12 cells) expressing an FGF-specific promoter construct (7xOCFRE) were used (G and J). Anosmin enhanced activities of FGF2, FGF4, and FGF8—2 in (G and J)—while the ECM proteins fibronectin (3), laminin-III (4), and collagen I (5) did not enhance FGF8 in (H). For BMP activity, a C2C12 cell line expressing a BMP-specific promoter (BRA) was used (H and K). Anosmin inhibited BMP5 and BMP7 activity (K). In contrast, the ECM proteins fibronectin and laminin-III enhanced BMP5 activity (H). For WNT activity, a C2C12 cell line expressing a WNT-specific promoter (TOPflash) was used (I). Anosmin inhibited WNT3a activity, while other ECM proteins were without effect (I). Data are shown as means and SEM. *$p < 0.05$. **$p < 0.01$.

(L) Western blotting of signaling molecules downstream of GF receptors. Purified anosmin protein- or BSA-soaked beads were implanted into the cranial region of $HH8^+$ embryos in ovo, and after 1–2 hr incubation at 38°C, the entire cranial region from six to seven embryos each were dissected and examined by western blotting. GAPDH was the control.

(M and N) Immunostaining of phosphorylated p38 in anosmin bead-treated embryo. Arrowheads indicate enhanced phosphorylated p38 (M) and increased phosphorylated p38 positive neural crest (N). Scale bar, 50 μm.

(O–R‴) Purified anosmin protein (red asterisk) and BSA as a control (black asterisk) were injected into the cranial region of $HH7^+$ embryos; asterisks in (O) and (P) indicate the sites of injection in the anterior midbrain region, and asterisks in (Q) and (R) indicate injection in the middle midbrain region. The embryos were cultured for 5 hr and then examined for *FGF8* and *SNAI2* expression by whole-mount in situ hybridization. Exogenous anosmin-enhanced *FGF8* and *SNAI2* expression levels at regions compared with internal control side and control BSA embryos (P-P′ and R-R‴, respectively). Scale bar, 150 μm in (O), (P), (Q), and (R) and 50 μm in (O′), (P′), (Q′, (R′), (R″), and (R‴).

See also Figure S4.

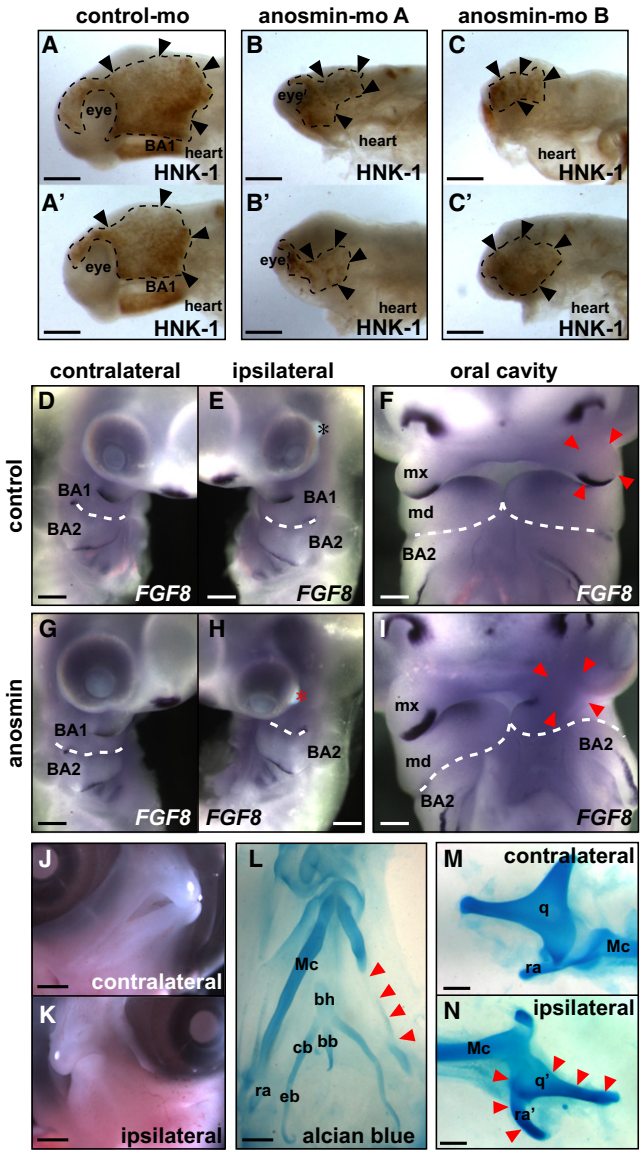

Figure 6. Anosmin Is Required for Cranial Neural Crest Differentiation and Normal Head Formation, and Exogenous Anosmin Alters Craniofacial Morphology

(A–C′) Whole-mount HNK-1 staining of control-mo- and two independent anosmin-mo-treated embryos. Electroporation of FITC-tagged mo was performed at HH4^{+}-5, and the embryos were cultured for 26 hr until HH12-13. Compared with the control embryos, indicated by arrowheads in (A) and (A′), migrating neural crest cells are severely reduced and head formation is defective in the anosmin-mo-treated embryos, indicated by arrowheads in (B), (B′), (C), and (C′). Scale bar, 200 μm.

(D–N) Purified-anosmin-coated or BSA-coated control beads were grafted in the cranial region at HH9 embryos in ovo, and the eggs were incubated for 3 more days until HH23 or for 8 days until HH35. *FGF8* expression was examined at HH23 (D–I), and alcian blue staining was performed at HH35 to visualize Meckel's cartilage (Mc), as shown in (L). Anosmin-treated embryos showed fusion of first and second BAs or reduced first BA, with loss of focal *FGF8* expression and increased diffuse *FGF8* expression (H and I, indicated by arrowheads). In most anosmin-treated embryos, the size of mouth became small compared with contralateral side (J and K), and Mc was absent (L, indicated by arrowheads) or quadrate (q) cartilage was smaller and retroarticular process was slightly bigger (N, indicated by arrowheads). bb, basibranchial; bh, basihyal; cb, ceratobranchial; eb, epibranchial; ra, retroarticular process. Scale bar, 250 μm in D–I, 1 mm in J–L, and 500 μm in M and N. See also Figure S5.

HH8-9 using whole-embryo culture for 5 hr. The embryos were examined for *FGF8* and *SNAI2* mRNA expression by whole-mount in situ hybridization. *FGF8* expression in the neural fold was enhanced by this experimental elevation of anosmin compared with BSA-injected control embryos (Figures 5P and 5P′, 5/5, arrowheads). Combining these gain-of-function findings with the anosmin knockdown results, our experiments indicate that anosmin regulates *FGF8* expression in the neural fold. Importantly, anosmin overexpression also enhanced expression of the neural crest marker *SNAI2* and resulted in increased numbers of *SNAI2*-positive cells in NFs on the injected side (Figures 5R–5R‴, 7/10, arrowheads). These results support the conclusion that anosmin promotes cranial neural crest formation.

Anosmin Is Required for Cranial Neural Crest Differentiation and Normal Head Formation

If the primary conclusion of this article is correct (i.e., that anosmin is essential for normal neural crest formation by modulating growth factors), there should be subsequent major effects on tissues derived from the neural crest in later-stage embryos. To evaluate this, mo-treated embryos were cultured for 26 hr from HH4^{+}-5 to HH12-13. Whole-mount immunostaining was then performed using the HNK-1 antibody, which recognizes a cell surface epitope on migrating neural crest cells (Tucker et al., 1984). In control-mo-treated embryos, wide regions of migrating neural crest cells were immunostained by the HNK-1 antibody as shown by the brown staining in Figures 6A and 6A′ (arrowheads). However, in anosmin-mo embryos, areas of HNK-1 immunoreactivity were severely decreased compared to controls (Figures 6B and 6B′, anosmin-mo A, 5/6, arrowheads; Figures 6C and 6C′, anosmin-mo B, 5/6, arrows). In addition to these deficits in neural crest, we also observed defects in head formation in anosmin-mo embryos compared to controls (Figures 6B–6C′) with reduced forebrain and eye primordium. These results indicate that anosmin is necessary for cranial neural crest cell development and normal craniofacial morphology.

Excess Anosmin Affects Craniofacial Morphology

Because our gain-of-function experiments indicated that exogenous anosmin can stimulate neural crest formation (Figure 5), we evaluated whether exogenous anosmin would alter later craniofacial development. Beads soaked with purified anosmin or bovine serum albumin (BSA) as a control were implanted into cranial regions of HH9^{-} embryos in ovo. We first confirmed that control BSA beads did not affect cranial neural crest formation (data not shown, 11/11) and that considerable anosmin protein remained intact even 24 hr after implantation (Figure S5A). The embryos were cultured for 3–8 days to examine for late effects on craniofacial morphology, specifically branchial arches (BAs) at 3 days (HH23) and Meckel's cartilage formation at 8 days (HH35). In normal embryogenesis, the maxillary and mandibular processes are formed separately, and both processes express *FGF8* on their edges (Figures 6D–6F,

arrowheads). In contrast, embryos treated with anosmin-beads displayed smaller maxillary and mandibular processes, with low or absent *FGF8* expression at HH23 (Figures 6H and 6I, 4/5, arrowheads). Excess anosmin also resulted in craniofacial malformations such as small mouth at HH35 (Figures 6J and 6K; 15/38 at 0.5 mg/ml anosmin) compared with 1/17 using control beads, or 4/14 at 2 μg/ml and 4/9 at 10 μg/ml anosmin (data not shown). Elevated anosmin inhibited formation of Meckel's cartilage (Figure 6L, 6/26, arrowheads) or abnormal quadrate cartilage and retroarticular process (Figure 6N, 7/26, arrowheads) according to alcian blue staining; it sometimes also resulted in ectopic or extra cartilage surrounding the oral cavity (mouth) and Meckel's cartilage (Figures S5B–S5D, 5/26, arrowheads). Taken together, our results suggest that normal levels of anosmin are important for normal craniofacial morphology.

DISCUSSION

In this study, we discovered strong differential gene expression of the ECM protein anosmin in the cranial neural crest by cDNA microarray analysis and qPCR. We found that anosmin is secreted by the cranial neural crest and established that it provides autocrine regulation of cranial neural crest formation. We also demonstrated that anosmin enhances FGF8 activity, while inhibiting both BMP5 and WNT3a activities. Depleting or locally enhancing levels of anosmin revealed its crucial role in neural crest formation, with rescue of anosmin depletion by an appropriate combination of growth factors. In addition, our studies suggest a model in which an ECM protein plays a regulatory role in generating cranial neural crest cells by positively and negatively governing growth factor activities during early embryonic development.

At early stages (HH3-4$^+$) before cranial neural crest formation, FGF8, BMP4 (but not BMP5), and WNT3a activities are required for neural crest specification, as well as gastrulation and neural induction (Streit et al., 2000; Yang et al., 2002; Monsoro-Burq et al., 2003; Marchant et al., 1998; García-Castro et al., 2002). In this study, we found that *BMP5* mRNA was first detectable at HH7 following neural crest specification and that its expression was strongly localized to the cranial neural crest. We confirmed the role of BMP5 in neural crest formation (data not shown) by injecting recombinant BMP5 protein (0.5–1.0 μM) into cranial regions of HH6-7 embryos. At HH8-9, this exogenous BMP5 strongly induced ectopic expression of the neural crest marker *MSX2* (in neural crest, neural plate, and surrounding tissues such as epidermis and mesenchyme) but strongly blocked *SNAI2* expression in cranial neural crest. These results, combined with the *BMP5* expression pattern, suggest that appropriate BMP5 activity is involved in normal cranial neural crest formation.

Depleting anosmin resulted in diminished expression of the well-studied neural crest formation genes *SNAI2*, *FOXD3* and *SOX9*, but not *PAX7*, and reduced neural crest differentiation. In contrast, local increases of anosmin promoted neural crest formation, with late effects on craniofacial morphology. Our findings establish that anosmin is a regulatory ECM protein that is involved in growth factor regulation and neural crest formation but not in neural crest specification.

How does anosmin function in neural crest/craniofacial development? It can both regulate gene expression of the key growth factors FGF8 and BMP5 and directly bind to FGF8, BMP5, and WNT3a as it governs their activities. A recent review by Hynes (2009) proposes the idea that highly conserved domains of ECM molecules are important for governing interactions and matrix-mediated presentation of growth factors to receptors. In fact, a recent study demonstrates that the ECM proteins fibrillin 1 and fibrillin 2 can differentially function to sequester BMP and/or TGF-β to reduce their functional bioavailability (Nistala et al., 2010). Although anosmin can suppress BMP5 (but not BMP4) and WNT3a activities, it has dual functionality in being able to stimulate FGF8 activity. The modulating or balancing effects of anosmin that we describe affect three growth factors—FGF, BMP, and WNT—that are key factors in neural crest formation and craniofacial development (Sauka-Spengler and Bronner-Fraser, 2008; Trainor et al., 2002; Shigetani et al., 2000).

Our in vivo and in vitro experiments suggest that anosmin functions as an enhancer of FGF signaling by promoting FGF8-FGFR1 complex formation through direct interaction with FGF8. Consistent with this idea, anosmin overexpressed in Chinese hamster ovary (CHO) cells increases FGFR1 accumulation on the cell membrane (Ayari and Soussi-Yanicostas, 2007). However, contrary to our findings, Hu and colleagues showed that anosmin suppresses FGFR1 accumulation and its signaling through direct binding to FGFR1 (Hu et al., 2009). But, similar to our results, Hu et al. also reported that anosmin binds to preformed FGF2-FGFR1 indirectly and, in turn, activates FGF signaling (Hu et al., 2009). One important methodological difference is that we generated our tag-free anosmin using mammalian cells, whereas Hu et al. (2009) used insect cells. Because insect cells produce different posttranslational protein modifications, the discrepancy between their results and ours may be explained by our use of anosmin produced by mammalian rather than insect cells.

Finally, could anosmin be involved in other early steps of embryonic development besides cranial neural crest formation? In this study, we showed that anosmin regulates *SNAI2* gene expression in cranial neural crest formation. However, SNAI1/2 is a key transcription factor involved not only in neural crest formation but also in regulating epithelial to mesenchymal transition (EMT) in cancer metastasis and developmental processes such as gastrulation (Thiery et al., 2009; Yang and Weinberg, 2008). Prevention of EMT and mesenchymal-to-epithelial transition (MET) is also crucial for normal embryonic developmental processes. For example, SOX2 is strongly expressed in the neural plate and promotes neural tube development by repressing *SNAI2* expression (Wakamatsu et al., 2004), SOX3 prevents gastrulation by suppressing *SNAI1/2* expression to maintain neural and nonneural ectoderm (Acloque et al., 2011), and *SOX2* and *SOX3* expression can be driven by FGF signaling (Mansukhani et al., 2005; Ciruna and Rossant, 2001; Acloque et al., 2011). Somitogenesis is a well-known example of MET converting presomitic mesenchymal cells to epithelial cells (Nakaya et al., 2004). Interestingly, we detected *anosmin* mRNA not only in NFs but also in Hensen's node at late gastrulation (HH4$^+$-6) and in migrating presomitic mesoderm before somitogenesis at HH7-9 (Figure 2). Moreover, we find

anosmin protein localized not only in neural fold but also in the entire neural plate (Figure 2). Since a balance of FGF, BMP, and WNT control EMT and MET during embryonic development (Dorey and Amaya, 2010; Heisenberg and Solnica-Krezel, 2008; Sylvie et al., 2011), it may be interesting to examine potential roles of anosmin in developmental processes involving transitions to epithelia and mesenchyme, such as gastrulation, neural tube development, and somitogenesis by regulating *SNAI1/2* and *SOX2/3*.

In summary, our findings provide evidence that an ECM protein in the cellular microenvironment can both negatively and positively coordinate regulatory growth factor activities at temporal and spatial levels to facilitate specific tissue differentiation during embryonic development.

EXPERIMENTAL PROCEDURES

Experimental Animals and RNA Isolation

Fertile chicken eggs were obtained from CBT Farms, Federalsburg, MD, USA, or Charles River Laboratories, North Franklin, CT, USA, and were incubated at 38°C in a humidified incubator. Embryos were staged according to the procedures of Hamburger and Hamilton (1951).

NFs and neural plates were dissected from HH stage 8 embryos using tungsten needles (Fine Science Tools) in ice-cold Hanks' balanced salt solution (HBSS, Invitrogen) supplemented with 1 mM $MgCl_2$, 1 mM $CaCl_2$, and 1 mM HEPES at pH 7.5. The isolated tissues were dissolved in TRIzol (Invitrogen), snap frozen in dry ice/ethanol, and then stored at −80°C overnight. Total RNA isolated according to the manufacturer's protocol was treated with DNase I (Sigma) at 37°C for 30 min.

Whole-Embryo Culture and MO Transfection

$HH4^+$ to 5 embryos were cultured dorsal side down spanning a hole in filter paper on egg white in a 35 mm culture dish covered by Parafilm as described previously with minor modifications (Chapman et al., 2001; Y.E., unpublished data). For electroporation, the embryos were placed into an electroporation chamber from Unique Medical Imada filled with HBSS. Fluorescein isothiocyanate (FITC)-labeled mo [Gene Tools, 0.5 to 1 mM morpholino mixed with 5 μg/μl empty pCAGGS plasmid (Momose et al., 1999) in HBSS] were injected on to the entire cranial neural ectoderm region of the embryos followed by two square-wave electroporation pulses (10 mV, 25 ms duration separated by 200 ms) using a CUY21 electroporator (Tokiwa Science). After electroporation, the embryo was placed in the 35 mm dish dorsal side down. The embryos were incubated within a moist glass dish at 38°C for 10–11 hr to HH8 or 26 hr to HH12-13. The antisense mo used were: standard control (5′-CCTCTTACC TCAGTTACAATTTATA-3′) and two different oligonucleotides for the chicken anosmin 5′UTR antisense (A: 5′-TGCTGCGGGCTGAGCTGCTGCTCGC-3′ and B: 5′-CAGCTCCGCGCCGCAGAAACTAAAC-3′) designed according to Rugarli et al. (1993).

Anosmin and Other Antibodies

Custom anosmin antibodies (HL6158, HL6157, and HL6308; see Supplemental Experimental Procedures) were produced (Covance). HL6158 and HL6157 antibodies were used for immunostaining and western blotting. For coimmunoprecipitation and ELISA, HL6157 and HL6308 antibodies were used. FGF8 and FGFR1 antibodies were from R&D Systems; and total p38, phospho-p38, total SMAD1, phospho-SMAD1/5/8, and total ERK1/2, phospho-ERK1/2 antibodies were from Cell Signaling Technology. HNK-1 and SNAI2 (62.1E6) antibodies were from the Developmental Studies Hybridoma Bank. Anti-fibronectin antibody (R745) was previously described (Cukierman et al., 2001).

In Situ Hybridization and Immunohistochemistry

In situ hybridization and immunohistochemistry on frozen sections and in whole mounts were performed as described previously (Endo et al., 2002), with minor modifications as described in Supplemental Experimental Procedures.

Cell Lines

Mouse melanoma cells (B16-F10, ATCC) and myoblasts (C2C12BRA from Dr. Daniel Rifkin; Zilberberg et al., 2007) were cultured in Dulbecco's modified Eagle's medium (DMEM) containing 10% fetal bovine serum (FBS), 100 U/ml penicillin, and 100 μg/ml streptomycin. For anosmin protein purification, B16-F10 cells were cultured in serumfree, antibioticfree DMEM (see Supplemental Experimental Procedures). For generating stable FGF or WNT reporter cell lines, wild-type mouse myoblasts C2C12 (ATCC) were transfected with an osteocalcin FGF response element (7xOCFRE) promoter/luciferase reporter (from Dr. Dwight Towler; Newberry et al., 1996) or TOPflash (Millipore) with pEF1-Neo (Invitrogen) using Lipofectamine 2000 (Invitrogen). The cells were selected in 600 μg/ml G418 (Mediatech) for 2 weeks, and they were transferred to G418-free medium 1 day before initiating experiments.

Growth Factors and Receptor-Binding Assay

Recombinant mouse or human FGF2, −4, −8, human BMP2, −4, −5, −7, and mouse WNT3a were from R&D Systems. For the receptor binding assay, recombinant FGF8 was preincubated with/without anosmin protein for 1 hr at room temperature in 0.1% BSA/Binding buffer (Invitrogen), and then FGFR1c-Fc (R&D Systems) was added for an additional hour. FGF8 bound to its receptor was detected by western blotting using anti-FGF8 or anti-FGFR1 antibodies (R&D Systems) after Dynabead protein G (Invitrogen) precipitation of the receptor or anosmin by HL6157 or HL6308 antibodies following the manufacturer's protocol.

Luciferase Reporter Assay

C2C12-7xOCFRE, -BRA, or -TOPflash cells were seeded in 96-well culture plates (Corning) at 4×10^3 cells/well. The cells were cultured in DMEM with 10% FBS and antibiotics. After 24 hr, the medium was replaced with serumfree 0.1% BSA (Sigma)/DMEM containing recombinant proteins (see previous paragraph) and purified extracellular matrix proteins as described for each experiment. After 18 hr (6 hr for the WNT assay), the cells were washed twice with PBS, and cells were lysed using 50 μl 1× Passive Lysis Buffer (Promega). Lysates were assayed for luciferase activity using the Luciferase Assay System from Promega and a Mithras LB 940 microplate reader (Berthold Technologies).

ACCESSION NUMBERS

The microarray data are deposited in GEO under series accession number GSE38381.

SUPPLEMENTAL INFORMATION

Supplemental Information includes five figures and Supplemental Experimental Procedures and can be found with this article online at http://dx.doi.org/10.1016/j.devcel.2012.07.006.

ACKNOWLEDGMENTS

We thank Dr. Woei-Jer Chuang for valuable advice on anosmin protein purification, members of the Yamada laboratory for comments, and Shelagh Johnson for proofreading. We especially thank Drs. Daniel Rifkin, Dwight Towler, and Angela Nieto for kindly providing C2C12-BRA cells, 7xOCFRE, and 3xOCFRE plasmids and chicken *SNAI2* plasmid, respectively. Supported by the Intramural Research Program of the National Institute of Dental and Craniofacial Research, National Institutes of Health. Y.E. was partially supported by the Japan Society for the Promotion of Science Research.

Received: November 3, 2011
Revised: April 3, 2012
Accepted: July 13, 2012
Published online: August 13, 2012

REFERENCES

Acloque, H., Ocaña, O.H., Matheu, A., Rizzoti, K., Wise, C., Lovell-Badge, R., and Nieto, M.A. (2011). Reciprocal repression between Sox3 and snail

transcription factors defines embryonic territories at gastrulation. Dev. Cell *21*, 546–558.

Ayari, B., and Soussi-Yanicostas, N. (2007). FGFR1 and anosmin-1 underlying genetically distinct forms of Kallmann syndrome are co-expressed and interact in olfactory bulbs. Dev. Genes Evol. *217*, 169–175.

Bailey, A.P., Bhattacharyya, S., Bronner-Fraser, M., and Streit, A. (2006). Lens specification is the ground state of all sensory placodes, from which FGF promotes olfactory identity. Dev. Cell *11*, 505–517.

Barembaum, M., Moreno, T.A., LaBonne, C., Sechrist, J., and Bronner-Fraser, M. (2000). Noelin-1 is a secreted glycoprotein involved in generation of the neural crest. Nat. Cell Biol. *2*, 219–225.

Basch, M.L., Bronner-Fraser, M., and García-Castro, M.I. (2006). Specification of the neural crest occurs during gastrulation and requires Pax7. Nature *441*, 218–222.

Chapman, S.C., Collignon, J., Schoenwolf, G.C., and Lumsden, A. (2001). Improved method for chick whole-embryo culture using a filter paper carrier. Dev. Dyn. *220*, 284–289.

Cheung, M., and Briscoe, J. (2003). Neural crest development is regulated by the transcription factor Sox9. Development *130*, 5681–5693.

Ciruna, B., and Rossant, J. (2001). FGF signaling regulates mesoderm cell fate specification and morphogenetic movement at the primitive streak. Dev. Cell *1*, 37–49.

Cukierman, E., Pankov, R., Stevens, D.R., and Yamada, K.M. (2001). Taking cell-matrix adhesions to the third dimension. Science *294*, 1708–1712.

Discher, D.E., Mooney, D.J., and Zandstra, P.W. (2009). Growth factors, matrices, and forces combine and control stem cells. Science *324*, 1673–1677.

Dorey, K., and Amaya, E. (2010). FGF signalling: diverse roles during early vertebrate embryogenesis. Development *137*, 3731–3742.

Dottori, M., Gross, M.K., Labosky, P., and Goulding, M. (2001). The winged-helix transcription factor Foxd3 suppresses interneuron differentiation and promotes neural crest cell fate. Development *128*, 4127–4138.

Endo, Y., Osumi, N., and Wakamatsu, Y. (2002). Bimodal functions of Notch-mediated signaling are involved in neural crest formation during avian ectoderm development. Development *129*, 863–873.

Engler, A.J., Sen, S., Sweeney, H.L., and Discher, D.E. (2006). Matrix elasticity directs stem cell lineage specification. Cell *126*, 677–689.

García-Castro, M.I., Marcelle, C., and Bronner-Fraser, M. (2002). Ectodermal Wnt function as a neural crest inducer. Science *297*, 848–851.

Hamburger, V., and Hamilton, H.L. (1951). A series of normal stages in the development of the chick embryo. J. Morphol. *88*, 49–92.

Hardelin, J.P., Julliard, A.K., Moniot, B., Soussi-Yanicostas, N., Verney, C., Schwanzel-Fukuda, M., Ayer-Le Lievre, C., and Petit, C. (1999). Anosmin-1 is a regionally restricted component of basement membranes and interstitial matrices during organogenesis: implications for the developmental anomalies of X chromosome-linked Kallmann syndrome. Dev. Dyn. *215*, 26–44.

Heisenberg, C.-P., and Solnica-Krezel, L. (2008). Back and forth between cell fate specification and movement during vertebrate gastrulation. Curr. Opin. Genet. Dev. *18*, 311–316.

Henderson, D.J., and Copp, A.J. (1997). Role of the extracellular matrix in neural crest cell migration. J. Anat. *191*, 507–515.

Hong, C.S., Park, B.Y., and Saint-Jeannet, J.P. (2008). Fgf8a induces neural crest indirectly through the activation of Wnt8 in the paraxial mesoderm. Development *135*, 3903–3910.

Hu, Y., Guimond, S.E., Travers, P., Cadman, S., Hohenester, E., Turnbull, J.E., Kim, S.H., and Bouloux, P.M. (2009). Novel mechanisms of fibroblast growth factor receptor 1 regulation by extracellular matrix protein anosmin-1. J. Biol. Chem. *284*, 29905–29920.

Hynes, R.O. (2009). The extracellular matrix: not just pretty fibrils. Science *326*, 1216–1219.

Inomata, H., Haraguchi, T., and Sasai, Y. (2008). Robust stability of the embryonic axial pattern requires a secreted scaffold for chordin degradation. Cell *134*, 854–865.

Le Douarin, N.M., and Kalcheim, C. (1999). The Neural Crest (Cambridge: Cambridge University Press).

Legouis, R., Hardelin, J.P., Levilliers, J., Claverie, J.M., Compain, S., Wunderle, V., Millasseau, P., Le Paslier, D., Cohen, D., Caterina, D., et al. (1991). The candidate gene for the X-linked Kallmann syndrome encodes a protein related to adhesion molecules. Cell *67*, 423–435.

Litsiou, A., Hanson, S., and Streit, A. (2005). A balance of FGF, BMP and WNT signalling positions the future placode territory in the head. Development *132*, 4051–4062.

Mansukhani, A., Ambrosetti, D., Holmes, G., Cornivelli, L., and Basilico, C. (2005). Sox2 induction by FGF and FGFR2 activating mutations inhibits Wnt signaling and osteoblast differentiation. J. Cell Biol. *168*, 1065–1076.

Marchant, L., Linker, C., Ruiz, P., Guerrero, N., and Mayor, R. (1998). The inductive properties of mesoderm suggest that the neural crest cells are specified by a BMP gradient. Dev. Biol. *198*, 319–329.

Mayor, R., Guerrero, N., and Martínez, C. (1997). Role of FGF and noggin in neural crest induction. Dev. Biol. *189*, 1–12.

Momose, T., Tonegawa, A., Takeuchi, J., Ogawa, H., Umesono, K., and Yasuda, K. (1999). Efficient targeting of gene expression in chick embryos by microelectroporation. Dev. Growth Differ. *41*, 335–344.

Monsoro-Burq, A.H., Fletcher, R.B., and Harland, R.M. (2003). Neural crest induction by paraxial mesoderm in Xenopus embryos requires FGF signals. Development *130*, 3111–3124.

Monsoro-Burq, A.H., Wang, E., and Harland, R. (2005). Msx1 and Pax3 cooperate to mediate FGF8 and WNT signals during Xenopus neural crest induction. Dev. Cell *8*, 167–178.

Nakaya, Y., Kuroda, S., Katagiri, Y.T., Kaibuchi, K., and Takahashi, Y. (2004). Mesenchymal-epithelial transition during somitic segmentation is regulated by differential roles of Cdc42 and Rac1. Dev. Cell *7*, 425–438.

Nelson, C.M., and Bissell, M.J. (2006). Of extracellular matrix, scaffolds, and signaling: tissue architecture regulates development, homeostasis, and cancer. Annu. Rev. Cell Dev. Biol. *22*, 287–309.

Newberry, E.P., Boudreaux, J.M., and Towler, D.A. (1996). The rat osteocalcin fibroblast growth factor (FGF)-responsive element: an okadaic acid-sensitive, FGF-selective transcriptional response motif. Mol. Endocrinol. *10*, 1029–1040.

Nieto, M.A., Sargent, M.G., Wilkinson, D.G., and Cooke, J. (1994). Control of cell behavior during vertebrate development by Slug, a zinc finger gene. Science *264*, 835–839.

Nistala, H., Lee-Arteaga, S., Smaldone, S., Siciliano, G., Carta, L., Ono, R.N., Sengle, G., Arteaga-Solis, E., Levasseur, R., Ducy, P., et al. (2010). Fibrillin-1 and -2 differentially modulate endogenous TGF-β and BMP bioavailability during bone formation. J. Cell Biol. *190*, 1107–1121.

Rogers, S.L., Bernard, L., and Weston, J.A. (1990). Substratum effects on cell dispersal, morphology, and differentiation in cultures of avian neural crest cells. Dev. Biol. *141*, 173–182.

Rugarli, E.I., Lutz, B., Kuratani, S.C., Wawersik, S., Borsani, G., Ballabio, A., and Eichele, G. (1993). Expression pattern of the Kallmann syndrome gene in the olfactory system suggests a role in neuronal targeting. Nat. Genet. *4*, 19–26.

Sakai, T., Larsen, M., and Yamada, K.M. (2003). Fibronectin requirement in branching morphogenesis. Nature *423*, 876–881.

Sauka-Spengler, T., and Bronner-Fraser, M. (2008). A gene regulatory network orchestrates neural crest formation. Nat. Rev. Mol. Cell Biol. *9*, 557–568.

Shigetani, Y., Nobusada, Y., and Kuratani, S. (2000). Ectodermally derived FGF8 defines the maxillomandibular region in the early chick embryo: epithelial-mesenchymal interactions in the specification of the craniofacial ectomesenchyme. Dev. Biol. *228*, 73–85.

Streit, A., Berliner, A.J., Papanayotou, C., Sirulnik, A., and Stern, C.D. (2000). Initiation of neural induction by FGF signalling before gastrulation. Nature *406*, 74–78.

Stuhlmiller, T.J., and García-Castro, M.I. (2012). FGF/MAPK signaling is required in the gastrula epiblast for avian neural crest induction. Development *139*, 289–300.

Sylvie, J., Ellen, C., and Kris, V. (2011). The role of Wnt in cell signaling and cell adhesion during early vertebrate development. Front. Biosci. *17*, 2352–2366.

Thiery, J.P., Acloque, H., Huang, R.Y.J., and Nieto, M.A. (2009). Epithelial-mesenchymal transitions in development and disease. Cell *139*, 871–890.

Trainor, P.A., Ariza-McNaughton, L., and Krumlauf, R. (2002). Role of the isthmus and FGFs in resolving the paradox of neural crest plasticity and prepatterning. Science *295*, 1288–1291.

Tucker, G.C., Aoyama, H., Lipinski, M., Tursz, T., and Thiery, J.P. (1984). Identical reactivity of monoclonal antibodies HNK-1 and NC-1: conservation in vertebrates on cells derived from the neural primordium and on some leukocytes. Cell Differ. *14*, 223–230.

Wang, X., Harris, R.E., Bayston, L.J., and Ashe, H.L. (2008). Type IV collagens regulate BMP signalling in Drosophila. Nature *455*, 72–77.

Wakamatsu, Y., Endo, Y., Osumi, N., and Weston, J.A. (2004). Multiple roles of Sox2, an HMG-box transcription factor in avian neural crest development. Dev. Dyn. *229*, 74–86.

Yamada, K.M., and Cukierman, E. (2007). Modeling tissue morphogenesis and cancer in 3D. Cell *130*, 601–610.

Yang, J., and Weinberg, R.A. (2008). Epithelial-mesenchymal transition: at the crossroads of development and tumor metastasis. Dev. Cell *14*, 818–829.

Yang, X., Dormann, D., Münsterberg, A.E., and Weijer, C.J. (2002). Cell movement patterns during gastrulation in the chick are controlled by positive and negative chemotaxis mediated by FGF4 and FGF8. Dev. Cell *3*, 425–437.

Zilberberg, L., ten Dijke, P., Sakai, L.Y., and Rifkin, D.B. (2007). A rapid and sensitive bioassay to measure bone morphogenetic protein activity. BMC Cell Biol. *8*, 41.

Zuzarte-Luís, V., Montero, J.A., Rodriguez-León, J., Merino, R., Rodríguez-Rey, J.C., and Hurlé, J.M. (2004). A new role for BMP5 during limb development acting through the synergic activation of Smad and MAPK pathways. Dev. Biol. *272*, 39–52.